Special Collection

Bromination Mechanism of *closo*-1,2-$C_2B_{10}H_{12}$ and the Structure of the Resulting 9-Br-*closo*-1,2-$C_2B_{10}H_{11}$ Determined by Gas Electron Diffraction

Josef Holub,[a] Yury V. Vishnevskiy,[b] Jindřich Fanfrlík,[c] Norbert W. Mitzel,*[b] Denis Tikhonov,[b] Jan Schwabedissen,[b] Michael L. McKee,[d] and Drahomír Hnyk*[a]

9-Br-*closo*-1,2-$C_2B_{10}H_{11}$ has been prepared and its gas-phase structure has been examined by means of gas electron diffraction. The structure of the carbaborane core is similar to the structure of the parent compound, which is of C_{2v} symmetry. A DFT-based search for the corresponding reaction pathway of the bromination of *closo*-1,2-$C_2B_{10}H_{12}$ revealed that the catalytic amount of aluminum reduces the barrier of the initial attack of the bromination agent toward the negatively charged part of the icosahedral carbaborane, i.e., the first transition state, from about 40 to about 27 kcalmol^{-1}. The Br–Br bond is weakened by an intermediate binding to the large π-hole on the aluminum atom of $AlBr_3$, which is the driving force for the $AlBr_3$-catalyzed bromination.

Electronic structures of polyhedral borane and heteroborane clusters are based on the presence of delocalized electron-deficient bonding.[1] Because of the aggregation of atoms, heteroborane is to form three-center, two-electron (**3c**–**2e**) bonds. The resulting trigonal faces are assembled to create three-dimensional shapes such as icosahedron and bicapped-square antiprism,[2] appearing in *closo* systems. Their molecular geometries can either be established in the solid state by X-ray diffraction or they can be computed for isolated free molecules.

Experimental molecular geometries of free *closo*-heteroboranes have been studied by employing the technique of gas-phase electron diffraction (GED).[2] In particular, attention was paid to 10-vertex bicapped square-antiprismatic[3,4] and 12-vertex icosahedral structural motifs.[5,6,7] Particular attention was focused on the heteroboranes based on *closo*-$B_{12}H_{12}^{2-}$; both vertex-substituted and *exo*-substituted icosahedrons were investigated by GED. The latter primarily include variously substituted *closo*-1,2-$C_2B_{10}H_{12}$. The main purpose of these examinations was to determine the structure of the icosahedral core C_2B_{10} more accurately because the scattering ability of C and B is almost the same.[8] Therefore, 9,12-X_2-*closo*-1,2-$C_2B_{10}H_{10}$ (X = I,[9] SH[10]) and 1,2-$(EH)_2$-*closo*-1,2-$C_2B_{10}H_{10}$ (E = S, Se)[11] have recently been structurally determined. In order to expand such structural studies, we have undertaken a gas-phase study of only a mono-substituted *closo*-1,2-$C_2B_{10}H_{12}$, i.e. 9-Br-*closo*-1,2-$C_2B_{10}H_{11}$, **1** (Figure 1). The main purpose of this structural examination is to explore the influence of a single externally (exo) positioned heteroatom on the carbaborane core. The structure of 1 has also been investigated in the solid state in light of the description of halogen bonding in brominated carbaboranes.[12]

The synthesis of **1** is based on the direct bromination of *closo*-1,2-$C_2B_{10}H_{12}$ with a catalytic amount of aluminum in carbon disulfide, a solvent with zero electric dipole moment.[13] In order to obtain a more detailed knowledge of this reaction, we also undertook a computational search for the corresponding reaction pathway, being armed with the results of the

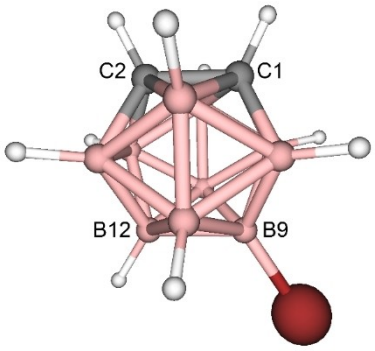

Figure 1. The molecular structure of **1**.

[a] Dr. J. Holub, Dr. D. Hnyk
Institute of Inorganic Chemistry of the Czech Academy of Sciences
CZ-250 68 Husinec – Řež (Czech Republic)
E-mail: hnyk@iic.cas.cz
[b] Dr. Y. V. Vishnevskiy, Prof. Dr. N. W. Mitzel, Dr. D. Tikhonov, Dr. J. Schwabedissen
Universität Bielefeld
Fakultät für Chemie
Anorganische Chemie und Strukturchemie
Universitätsstraße 25, 33615 Bielefeld (Germany)
E-mail: mitzel@uni-bielefeld.de
[c] Dr. J. Fanfrlík
Institute of Organic Chemistry and Biochemistry of the Czech Academy of Sciences
CZ-16610 Praha 6 (Czech Republic)
[d] Prof. Dr. M. L. McKee
Department of Chemistry and Biochemistry
Auburn University
Auburn, Alabama 36849 (USA)

Supporting information for this article is available on the WWW under https://doi.org/10.1002/cplu.202000543

This article is part of a Special Collection on "Chemistry in the Czech Republic".

bromination of *closo*-$B_{12}H_{12}^{2-}$, which occurs without the addition of any catalytic components.[14]

In the first step, it was necessary to find a bromination agent when aluminum was present in the reaction mixture. It is highly likely that aluminum forms aluminum tribromide, $AlBr_3$, in situ in the presence of elemental bromine, Br_2, and that $AlBr_3$ dimerizes to Al_2Br_6, which is quite resistant to CS_2.

On this basis, a complex of Br–Br···$AlBr_3$ could provide a good model for the bromination agent. Indeed, the computed electrostatic potential (ESP) molecular surfaces of Br_2, $AlBr_3$ and Br–Br···$AlBr_3$ supported this assumption. A driving force of this kind of bromination is the highly positive π-hole on the aluminum atom of $AlBr_3$ with the maximum value of the ESP on the molecular surface ($V_{S,max}$) of 78.8 kcal mol^{-1}, which is more than twice as large as that of BBr_3.[15] The π-hole interacts with a ring of the negative ESP on the molecular surface of Br_2 and the Br–Br bond in the resulting complex is lengthened from 2.34 to 2.41 Å and thus weakened, as computed at the B97D/cc-pVDZ/D3 level, with D3 being decisive for the Br_2···$AlBr_3$ complex. It is the σ-hole on the bromine atom that causes the attraction of the negative part of the carbaborane core (see Figure 2). Note that the dissociation of Al_2Br_6 into two molecules of $AlBr_3$ consumes 5.6 kcal mol^{-1}, whereas the formation of a contact ion pair $(AlBr_2)^+(AlBr_4)^-$ would be energetically more demanding, i.e. 81.2 kcal mol^{-1} in CS_2 (see SI for computational details). Interestingly, if the second Br_2 molecule serves as a catalyst, the first barrier is computed to be about 39 kcal mol^{-1} (the SMD model of the CS_2 solvent at the B3LYP/6-311 + G(2d,p) level with zero-point, heat-capacity, and entropy corrections with frequencies at the B3LYP/6-31 + G(d) level).

We have also investigated the bromination of other B–H vertices of *closo*-1,2-$C_2B_{10}H_{12}$, but those related to antipodally coupled atoms with carbon atoms, i.e. B(9,12), have turned out to be the most favorable – see the barriers of TS1 (Figure S1 in the Supporting Information) in relation to the different attacks of the bromination agent. Note that bromination under electrophilic conditions does not occur at all in positions B(3,6), which is in agreement with the highest barrier of the first transition state as shown in this figure. This agrees with the experimentally determined dipole moment of *closo*-1,2-$C_2B_{10}H_{12}$, which points from the middle of the C–C vector toward the center of the cluster.[16] The Br–Br bond is substantially lengthened in TS1cat (2.87 Å) as compared with it in Br_2 (2.34 Å), which is the geometrical reason for the initiation of the reaction.

Whereas Figure 3 illustrates the stationary points of the $AlBr_3$-catalyzed bromination with Br–Br···$AlBr_3$, Figure 4 depicts those where the second Br_2 molecule was considered to serve as a catalyst and Br–Br···Br–Br thus acts as the bromination agent. Note that the computed σ-hole (B97D/cc-pVDZ level) on Br rose from 28.9 to 33.7 kcal mol^{-1} when going from single Br_2 (Figure 2a) to Br–Br···Br–Br (Figure 2c). Such an increase might be viewed as the reason for the more favorable initial attack of Br–Br···Br–Br on the negatively charged region of *closo*-1,2-$C_2B_{10}H_{12}$ in relation to Br_2 only. Indeed, it is evident from Figure 5 and mainly from Figure 6 that the modeled non-catalyzed bromination of the icosahedral carbaborane, i.e. only with Br_2, has the highest barrier among these three pathways. Moreover, they represent the only existing pathways of the bromination under electrophilic conditions. The smallest difference between reactants and the first transition state occurs in the $AlBr_3$-catalyzed reaction pathway, with the first TS of the Br_2-catalyzed reaction pathway lying between the non-catalyzed and $AlBr_3$-catalyzed reaction pathways. Like in the case of the $AlBr_3$-catalyzed reaction, the Br–Br bond of the brominating Br_2 molecule is considerably lengthened in TS1Br_2cat (2.81 Å see Figure 4). In addition to that, the initial barrier of the non-catalyzed bromination, ca. 50.0 kcal mol^{-1} (see Figure 6), is very close to that of the monobromination of 1-Br-*closo*-$B_{12}H_{11}^{2-}$, 45.9 kcal mol^{-1}.[14] This hypothetical non-catalyzed reaction would occur in two steps. In the first step, the Br–Br bond breaks. One bromine atom is added to boron, while the second

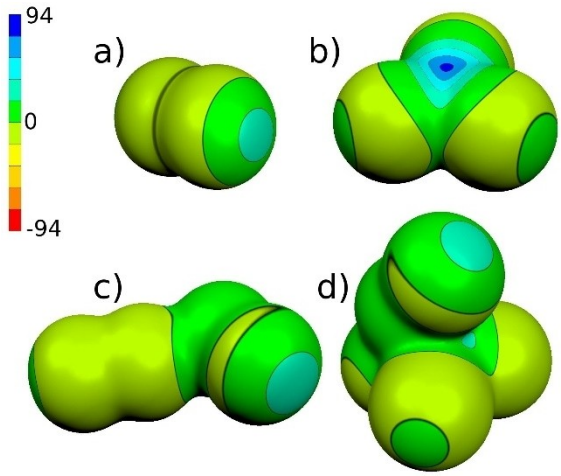

Figure 2. The electrostatic potential (ESP) molecular surface of a) Br_2, b) $AlBr_3$, c) Br_2···Br_2 and d) Br_2···$AlBr_3$ computed at the BD97/cc-pVDZ/D3 level. The ESP scale is in kcalmol^{-1}.

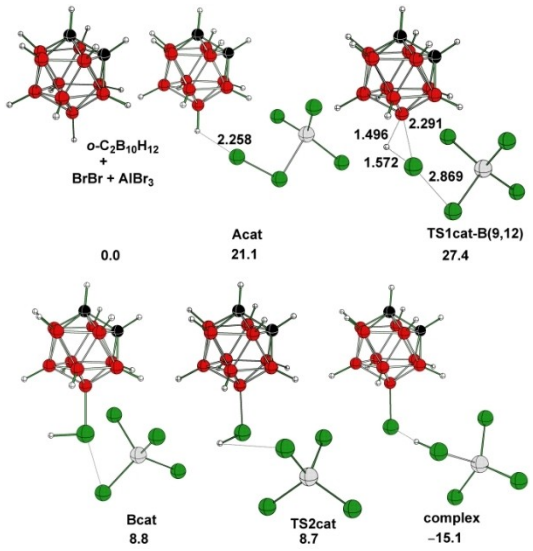

Figure 3. Stationary points of the $AlBr_3$-catalyzed bromination of boron vertices antipodally coupled with C1 and C2. Carbon atoms are in black, boron atoms are in orange, bromine atoms are in green, and the aluminum atom is in gray.

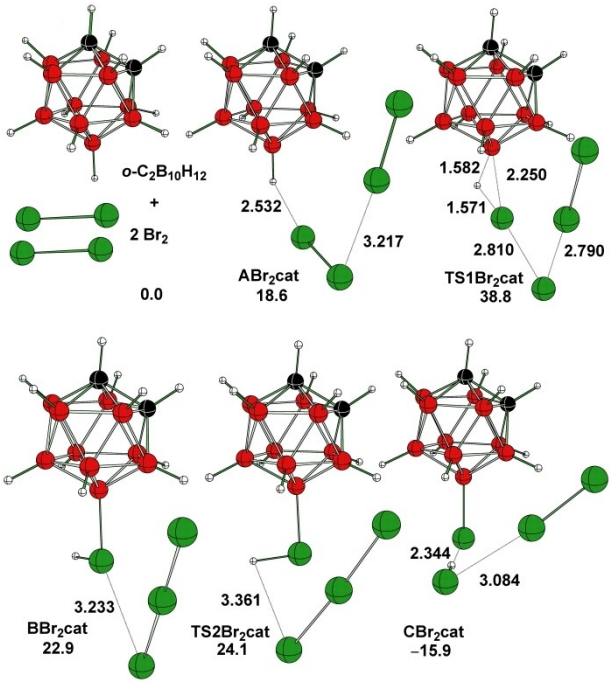

Figure 4. Stationary points of the bromination in which the second Br_2 molecule acts as a catalyst. Carbon atoms are in black, boron atoms are in orange, and bromine atoms are in green.

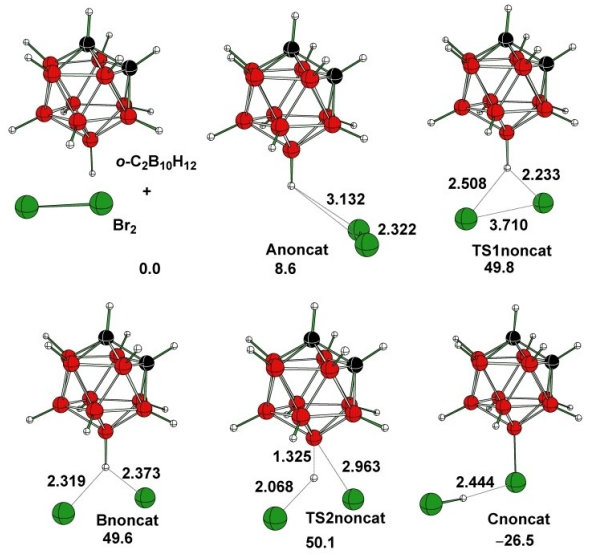

Figure 5. Stationary points of the non-catalyzed bromination of boron vertices antipodally coupled with C1 and C2. Carbon atoms are in black, boron atoms are in orange, and bromine atoms are in green.

bromine atom abstracts a hydrogen atom, as shown in Figure 5. Furthermore, there is a very shallow minimum and then another TS before reaching the Cnoncat stationary point, see Figures 5 and 6. Table S1 summarizes all the results for each reaction that was examined. These findings are in agreement with the experimental observations, also showing that the complex of $[Br_3]^-$ with hexamethylbenzene exists,[17] likewise in analogy with the stationary point BBr_2cat, shown in Figure 4.

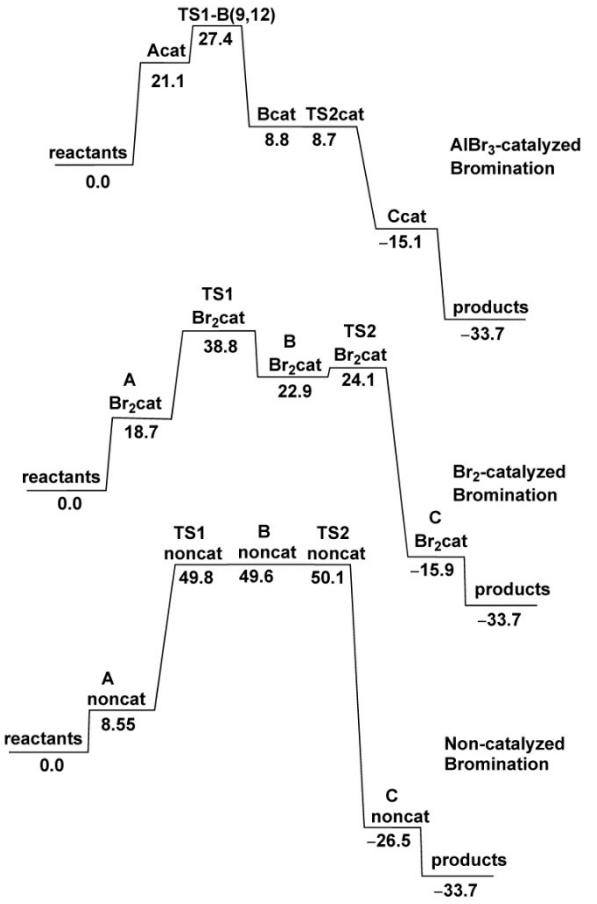

Figure 6. Stationary points of the potential energy surfaces of these three kinds of bromination of *closo*-1,2-$C_2B_{10}H_{12}$. $\triangle G$(298 K,CS_2) relative energies (in kcalmol^{-1}) using the SMD model of the CS_2 solvent at the B3LYP/6-311 + G (2d,p) level and zero-point, heat-capacity, and entropy corrections with frequencies at the B3LYP/6-31 + G(d) level.

Halogenation under similar conditions (i.e. with a catalytic amount of $AlCl_3$) has been reported for the 10-vertex *closo*-1,2-$C_2B_8H_{10}$ carborane. In the case of bromination, the reaction yielded the dibromo-derivative 7,10-Br_2-*closo*-1,2-$C_2B_8H_8$ product.[18]

The structure of compound **1** has been studied by means of gas electron diffraction (GED), and its semi-experimental molecular structure was refined from the obtained diffraction patterns using the UNEX program.[19] For experimental conditions, see Table S2. The refinement was performed in Cartesian coordinates, where additional regularization was applied to stabilize the solution of the inverse problem. Details of this method have been published in a recent paper.[11] Theoretical values of Cartesian coordinates from the MP2(fc)/SDB-cc-pVTZ calculation were used for regularization. The refined and predicted theoretical values of geometrical parameters for **1** are collected in Table 1. Additionally, the contributions *w* of experimental GED data into refined parameters were calculated using a recently proposed method.[11] Note that there is an overall agreement with the solid-state structure already reported,[12] e.g. C1–C2 in the solid state and gas phase have been determined as 1.615(7) and 1.635(2) Å, respectively.

Table 1. Selected theoretical and semi-experimental geometrical parameters [Å, degrees] of **1**.

Parameter[a]	MP2 r_e	GED r_e	r_g	w[b]
r(C–C)	1.621	1.619(2)	1.635(2)	0.59
r(C–B)	1.705	1.701(2)	1.717(2)	0.67
r(B–B)	1.781	1.775(2)	1.790(2)	0.73
r(B–Br)	1.938	1.936(1)	1.946(1)	0.91
r(C–H)	1.079	1.084(2)	1.105(2)	0.00
r(B–H)	1.180	1.185(2)	1.207(2)	0.00
∠(C–C–B)$_{narrow}$	61.8	61.9(1)		0.01
∠(C–C–B)$_{wide}$	111.8	111.6(1)		0.03
∠(C–B–C)	56.3	56.3(1)		0.02
∠(C–B–B)$_{narrow}$	58.4	58.5(1)		0.05
∠(C–B–B)$_{wide}$	103.9	103.9(1)		0.05
∠(B–C–B)$_{narrow}$	63.1	63.0(1)		0.07
∠(B–C–B)$_{wide}$	116.0	116.0(1)		0.09
∠(B–B–B)$_{narrow}$	60.0	60.0(1)		0.03
∠(B–B–B)$_{wide}$	108.1	108.1(1)		0.07
∠(B–B–Br)	121.6	121.7(1)		0.05
∠(C–C–H)	116.0	116.0(2)		0.00
∠(B–B–H)	123.4	123.4(1)		0.01
∠(C–B–H)	117.9	117.8(1)		0.01
∠(B–C–H)	118.3	118.4(1)		0.01
R-factor [%]		4.7		

[a] Averaged values are given, except for unique parameters. The numbers in parentheses are standard deviations from least-squares analysis. [b] The contributions of experimental GED data to refined parameters.

The refined molecular structure of **1** fits the experimental GED data well as shown by the relatively small R-factor of 4.7 %. The radial distribution functions (Figure 7) also exhibit good agreement between the model and the experimental data, although some small deviations have remained in the region of 4.5–5.5 Å. This can be attributed to inaccuracies in the calculated vibrational amplitudes and neglected asymmetry parameters. A complete investigation of the problem would require experimental gas-phase vibrational spectra, which were not available for this compound. However, the positions of the peaks in the model and experimental P(r) are in good agreement. Therefore, these peculiarities should not contribute to systematic errors in refined geometrical parameters.

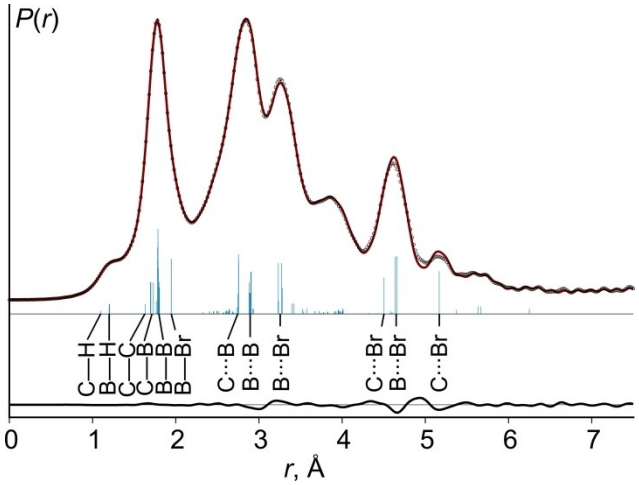

Figure 7. Experimental (dots) and model (line) radial distribution functions of **1**. The line below is the difference between the experiment and the model. The vertical bars show the contributions of atom pairs to diffraction patterns.

The refined parameter values are influenced by the extent to which they originate from experimental GED data (see the values w in Table 1). As expected, the largest values are those for the bond lengths C–C, C–B, B–B and B–Br. For the other parameters, especially for those containing hydrogen atoms, the w-values were very small. Accordingly, it makes sense to discuss only the parameters that have been primarily refined on the basis of experimental GED data (i.e. those with large w-values). The structure of the carbaborane core does not show any pronounced deviations from the C_{2v} symmetry, which is adopted by the parent *closo*-1,2-$C_2B_{10}H_{12}$,[9,10] although the overall symmetry of **1** is C_s. The presence of a bromine atom, with its much higher ability to scatter electrons, ensures much better structural characterization of the C_2B_{10} icosahedral core than the GED study of the parent *closo*-1,2-$C_2B_{10}H_{12}$ itself.[8]

In summary, we have prepared 9-Br-*closo*-1,2-$C_2B_{10}H_{11}$ and determined its gas-phase structure; the internal coordinates of the C_2B_{10} core differ only negligibly from those in the parent *closo*-1,2-$C_2B_{10}H_{12}$, in which e.g. r_{h1}(C–C) is 1.624(8) Å.[8] In order to understand the reaction pathway in which this monobrominated carbaborane originates, we have searched for such a mechanism computationally as well and found a similarity with the bromination mechanism for benzene, where a catalytic amount of aluminum or AlX_3 (X = Cl, Br) is also needed for the bromination to occur.[20] The electronic energy of the second experimentally available monobromo *closo*-1,2-$C_2B_{10}H_{11}$, i.e. 3-Br-*closo*-1,2-$C_2B_{10}H_{11}$,[21] obtained in a synthetic procedure that entirely differs from the preparation of **1**, is lower than that of **1** by 1.7 kcal mol^{-1} as computed at the B3LYP/6-31 + G(d) level. However, **1** appeared to be more stable than 3-Br-*closo*-1,2-$C_2B_{10}H_{11}$ by 2.6 kcal mol-1 when the corresponding free energies were taken into account (see e.g. Figure 6 for computational details).

Acknowledgements

We thank the Czech Science Foundation for financial support (project no. 19-17156S). This work was funded by the Deutsche Forschungsgemeinschaft (DFG) (grant VI 713/1-2 for YuVV, project no. 243500032) and through the core facility GED@BI (grant MI477/35-1 for NWM, project no. 324757882). MLM thanks Auburn University for access to the HOPPER computer. Open access funding enabled and organized by Projekt DEAL.

Conflict of Interest

The authors declare no conflict of interest.

Keywords: bromination · carboranes · electron diffraction · reaction pathways · transition states

[1] See e.g. K. Wade, *Electron Deficient Compounds*, Nelson, London, 1971.
[2] D. Hnyk, D. A. Wann in *Boron*: *The Fifth Element* (D. Hnyk, M. L. McKee, Eds.): *Challenges and Advances in Computational Chemistry and Physics* 2016, 20, 17–48.
[3] D. Hnyk, D. W. H. Rankin, H. E. Robertson, M. Hofmann, M. Bühl, P. v. R. Schleyer, *Inorg. Chem.* **1994**, *33*, 4781–4786.
[4] D. Hnyk, D. A. Wann, J. Holub, S. Samdal, D. W. H. Rankin, *Dalton Trans.* **2011**, *40*, 5734–5737.
[5] D. Hnyk, E. Vajda, M. Bühl, P. v. R. Schleyer, *Inorg. Chem.* **1992**, *31*, 2464–2467.
[6] D. Hnyk, M. Bühl, P. v. R. Schleyer, H. V. Volden, S. Gundersen, J. Müller, P. Paetzold, *Inorg. Chem.* **1993**, *32*, 2442–2445.
[7] D. Hnyk, D. A. Wann, J. Holub, M. Bühl, H. E. Robertson, D. W. H. Rankin, *Dalton Trans.* **2008**, 96–100.
[8] A. R. Turner, H. E. Robertson, K. B. Borisenko, D. W. H. Rankin, M. A. Fox, *Dalton Trans.* **2005**, 1310–1318.
[9] Y. V. Vishnevskiy, D. S. Tikhonov, C. G. Reuter, N. W. Mitzel, D. Hnyk, J. Holub, D. A. Wann, P. D. Lane, R. J. F. Berger, S. A. Hayes, *Inorg. Chem.* **2015**, *54*, 11868–11874.
[10] D. A. Wann, P. D. Lane, H. E. Robertson, T. Baše, D. Hnyk, *Dalton Trans.* **2013**, *42*, 12015–12019.
[11] T. Baše, J. Holub, J. Fanfrlík, D. Hnyk, P. D. Lane, D. A. Wann, Y. V. Vishnevskiy, D. Tikhonov, C. G. Reuter, N. W. Mitzel, *Chem. Eur. J.* **2019**, *25*, 2313–2321.
[12] J. Fanfrlík, J. Holub, Z. Růžičková, J. Řezáč, P. D. Lane, D. A. Wann, D. Hnyk, A. Růžička, P. Hobza, *ChemPhysChem* **2016**, *17*, 3373–3376.
[13] J. Plešek, T. Hanslík, *Collect. Czech. Chem. Commun.* **1973**, *38*, 335–337.
[14] M. Lepšík, M. Srnec, D. Hnyk, B. Grüner, J. Plešek, Z. Havlas, L. Rulíšek, *Collect. Czech. Chem. Commun.* **2009**, *74*, 1–27.
[15] J. Macháček, M. Bühl, J. Fanfrlík, D. Hnyk, *J. Phys. Chem. A* **2017**, *121*, 9631–9637.
[16] D. Hnyk, V. Všetečka, L. Drož, O. Exner , *Collect. Czech. Chem. Commun.* **2001**, *66*, 1375–1379.
[17] A. V. Vasilyev, S. V. Lindeman, J. K. Kochi, *New J. Chem.* **2002**, *26*, 582–592.
[18] M. Bakardjiev, A. Růžička, Z. Růžičková, J. Holub, O. L. Tok, B. Štíbr, *Inorg. Chem.* **2017**, *56*, 5971–5975.
[19] Yu. V. Vishnevskiy, 2020, UNEX version 1.6, http://unexprog.org (accessed Jun 23, 2020).
[20] P. Vollhard, N. Shore, in *Org. Chem.: Structure and Function*, 5th Ed., New York: Freeman and Company 2007.
[21] J. Li, M. Jones, Jr., *Inorg. Chem.* **1990**, *29*, 4162–4163.

Manuscript received: July 23, 2020
Revised manuscript received: August 18, 2020
Accepted manuscript online: August 26, 2020